Cell and Tissue Research (2026) 405:2
https://doi.org/10.1007/s00441-026-04081-6

RESEARCH

Gill ionocytes of the Lake Magadi tilapia (*Oreochromis Alcolapia grahami*), an extremophilic teleost native to a highly alkaline environment

Jonathan M. Wilson[1] · Chris M. Wood[2,3,4] · Pierre Laurent[4] · Claudine Chevalier[4] · Patrícia G. Ferreira[5] · Kevin V. Brix[3] · Gudrun DeBoeck[6] · Harold L. Bergman[7] · Adalto Bianchini[8] · Lucas Feijó Bianchini[8] · John N. Maina[9] · Ora E. Johannsson[2,10] · Geraldine D. Kavembe[11] · Michael B. Papah[11] · Rodi O. Ojoo[12]

Received: 21 January 2026 / Accepted: 28 May 2026
© The Author(s), under exclusive licence to Springer-Verlag GmbH Germany, part of Springer Nature 2026

Abstract

The Magadi tilapia thrives in arguably the most extreme aquatic environment on earth for fish, the hot springs of Lake Magadi in Kenya with its severe water chemistry: pH 10, alkalinity 300 mEq·L^{-1}. This fish is 100% ureotelic yet has an osmoregulation pattern typical of marine teleosts, although the dominant water anion is HCO_3^- rather than Cl^-. The gills must actively export base equivalents ($HCO_3^- + CO_3^{2-}$) and Na^+ against strong electrochemical gradients, yet simultaneously take up Cl^-, for which a hypothetical "Laurent model" based on ionocyte structure alone was proposed. This model has been tested using immunohistochemistry to characterize ionocyte types based on ion transport protein expression patterns [CFTR anion channel, Na^+:K^+:2Cl- cotransporter (NKCC)/Na^+:Cl^- cotransporter (NCC), Na^+:HCO_3^- co-transporter (NBC), Na^+/K^+-ATPase (NKA), and urea transporter (UT)]. A typical "seawater ionocyte" (Type IV) with apical CFTR and basolateral NKCC1 and NKA, is present validating key elements of the model. A "freshwater ionocyte" (Type II) is also present (apical NCC, weaker NKA and strong NBCe1 basolateral staining). A third Type I ionocyte with only NKA staining was also identified. An acid excreting Type III ionocyte (apical NHE3 and basolateral NKA) was not present. The Magadi tilapia is unusual in having co-expression of both Type IV and Type II ionocytes, which are typically associated with Cl^- excretion and uptake, respectively. Instead, we propose Type IV ionocytes are involved in base equivalent and Na^+ excretion and Type II ionocytes in Cl^- uptake. In these ureotelic fishes, the UT occurs only in lamellar pavement cells.

Keywords Na^+:HCO_3^- co-transporter (NBC) · Cystic fibrosis transmembrane regulator (CFTR) · Na^+:K^+:$2Cl^-$ cotransporter (NKCC) · Na^+:Cl^- cotransporter (NCC) · Brackish water

Pierre Laurent has passed away.

✉ Jonathan M. Wilson
jmwilson@wlu.ca

[1] Dept. of Biology, Wilfrid Laurier University, Waterloo, ON N2L 3C5, Canada

[2] Dept. of Zoology, University of British Columbia, Vancouver, B.C. V6T 1Z4, Canada

[3] Dept. of Marine Biology and Ecology, Rosenstiel School of Marine, Atmospheric and Earth Science, University of Miami, Miami, FL 33149, USA

[4] Dept. of Biology, McMaster University, Hamilton, ON L8S 4K1, Canada

[5] Dept. of Biology, University of Ottawa, Ottawa, ON K1N 6N5, Canada

[6] Dept. of Biology, University of Antwerp, Antwerp, Belgium

[7] Dept. of Zoology and Physiology, University of Wyoming, Laramie, WY 82071, USA

[8] Instituto de Ciências Biológicas, Universidade Federal Do Rio Grande (FURG), Rio Grande, RS 96201-900, Brazil

[9] Dept. of Zoology, University of Johannesburg, Johannesburg, South Africa

[10] Great Lakes Laboratory for Fisheries and Aquatic Sciences, Dept. of Fisheries and Oceans, Burlington, ON, Canada L7R 4A6, Canada

[11] Dept. of Range and Wildlife Sciences, Southeastern University College, Kitui 170-90200, Kenya

[12] Dept. of Veterinary Anatomy and Physiology, University of Nairobi, Nairobi, Kenya

Published online: 23 June 2026

Introduction

The Magadi tilapia, with a current taxonomic name of *Oreochromis (Alcolapia) grahami* as recommended by Ford et al. (2019) (formerly *Alcolapia grahami*, formerly *Oreochromis alcalicus grahami*, formerly *Sarotherodon alcalicus grahami*, formerly *Tilapia grahami*) lives in arguably the most extreme aquatic environment on earth for fish, Lake Magadi in the Rift Valley of Kenya. In addition to water temperatures up to 45 °C, it survives extreme night-time hypoxia and anoxia, daytime hyperoxia, and some of the highest levels of reactive oxygen species (ROS) that have ever been recorded in natural waters (Coe 1966; Narahara et al. 1996; Johannsson et al. 2014; Wood et al. 2016). However, its greatest challenge may be the highly unusual water chemistry in the hot springs where it lives around the edges of Lake Magadi.

Tables listing the compositions of Lake Magadi water and the plasma of *O.A. grahami* can be found in Eddy et al. (1981), Eddy and Maloiy (1984), Wood et al. (1989), Laurent et al. (1995), Wood et al. (2002a), Wood et al. (2002b), Wilson et al. (2004), and Wood et al. (2012). Water values vary seasonally and among hot springs. However, the water pH is typically about 10 due to very high concentrations of HCO_3^- and CO_3^{2-} resulting in an alkalinity over 300 mmol·L^{-1} at times and osmolality of about 500–600 mOsm·kg^{-1}. By way of comparison, the typical pH of seawater is about 8, its alkalinity is 2–3 mmol·L^{-1} and its osmolality is about 1050 mOsm kg^{-1}. Moreover, unlike seawater where Na^+ and Cl^- concentrations are both high (450–550 mmol·L^{-1}), Lake Magadi water has Na^+ concentrations (~356 mmol·L^{-1}) that are ~threefold greater than Cl^- concentrations (~110 mmol·L^{-1}), because the alkaline anions (HCO_3^- and CO_3^{2-}) account for most of the negative charge. Surprisingly, the Magadi tilapia is able to maintain a plasma ionic composition and osmolality at levels that are very similar to those of typical teleosts in seawater.

Another particularly striking characteristic is that these fish excrete only urea and no ammonia, presumably an adaptation to the difficulty of excreting ammonia against a large pH gradient; *O.A. grahami* is the only 100% ureotelic teleost (Randall et al. 1989; Wood et al. 1989; Lindley et al. 1999). A specific facilitated diffusion urea transporter in Magadi tilapia (mtUT) has been cloned from the gills and tentatively localized to the pavement cells based on the presence of similar vesicles found in the gills of facultatively ureogenic Gulf toadfish (*Opsanus beta*) by transmission electron microscopy (TEM) (Laurent et al. 2000; Walsh et al. 2001). UT localization has been confirmed by IHC in the Gulf toadfish (Bucking et al. 2013).

It has proven difficult to accurately measure the blood acid–base status in such small fish (typically < 5 g), but plasma pH and HCO_3^- concentrations appear to be elevated above values typical of other teleosts at comparable temperature (Johansen et al. 1975; Wood et al. 1994, 2002b, 2012). This undoubtedly reflects the extreme alkalinity of the environment, which makes the water a "CO_2 vacuum" that renders the retention of dissolved CO_2 in the blood virtually impossible, while simultaneously presenting very high concentrations of base equivalents to the external gill surface. Furthermore, in order to maintain body hydration in this hyperosmotic environment, Magadi tilapia drink the external water at a high rate (Maloiy et al. 1978; Wood et al. 2002a; Bergman et al. 2003). However, rather than using the intestinal transport of Na^+ and Cl^- to drive the absorption of the water in the manner of seawater teleosts, instead they transport Na^+ and mainly HCO_3^- or CO_3^{2-}, rather than Cl^- in order to absorb water across the gut epithelium (Bergman et al. 2003). Thus, the influx of base equivalents occurs at both intestine and gills.

Detailed analyses of the electrochemical gradients across the gills have demonstrated that there is a very strong net gradient driving base equivalents inwards, a modest net gradient driving Na^+ inwards, and a smaller net gradient driving Cl^- outwards (Eddy et al. 1981; Wood et al. 2012). Passive permeability of the gills to HCO_3^- is unusually low, which is presumably adaptive to reduce the loading of base equivalents (Wood et al. 2012). Nevertheless, the cells are tasked with the unusual situation of excreting base equivalents to the environment against a steep electrochemical gradient, while simultaneously excreting Na^+ yet taking up Cl^-. The transepithelial potential (TEP) is inside positive, that results from an inwardly directed Na^+ diffusion potential upon which is superimposed an electrogenic component thought to result from the secondary active export of base equivalents (Wood et al. 2012). In standard marine teleosts, the TEP is also positive inside, but the electrogenic component results from the secondary active export of Cl^- rather than base equivalents (Potts 1984; Potts and Hedges 1991).

There have been numerous morphological studies on the gill ionocytes using classical techniques (light, scanning, and TEM microscopy; Maina 1990, 1991; Laurent et al. 1995; Wood et al. 2002a, 2013; DeBoeck et al. 2019). Some of these studies suggest that more than one type of ionocyte is present, but the general picture that has emerged is that most of the ionocytes have a typical seawater morphology and location. These cells are rich in mitochondria with a complex tubular network penetrating the cytoplasm from the basolateral surface and are recessed at the bases of pits bordered by partially overlying pavement cells and flanked by interdigitating accessory cells. Based only on the morphology of these ionocytes, Laurent et al. (1995) proposed a scheme of passive Na^+ export through the paracellular 'shunt' pathway (between ionocytes and accessory cells) energized by the secondary active excretion of base equivalents through the

transcellular pathway into the apical crypts. This would be powered by basolateral Na^+/K^+-ATPase, with base equivalents entering the cell through a basolateral co-transporter analogous to NKCC (Na^+:K^+:2Cl^- cotransporter) and leaving apically through anion channels. The scheme was a modification of the classic "chloride cell" model of Silva et al. (1977), but with base equivalents replacing Cl^- at every step. Later electrophysiological data (Wood et al. 2012) supported this model. Additionally, Laurent et al. (1995) proposed that Cl^- uptake occurred via an apical Cl^-/HCO_3^- exchanger in these cells.

Immunohistochemistry (IHC) is a powerful tool to characterize ionocytes beyond the information provided by structure (Dymowska et al. 2012; Hiroi and McCormick 2012; Wilson 2007). However, with the exception of its use in localizing ammonia transporters (Wood et al. 2013), this technique has not been applied to the gills of *O.A. grahami*. In other tilapine fishes, IHC has identified three (Dymowska et al. 2012) or four types (Hiroi et al. 2005, 2008; Choi et al. 2011; Hiroi and McCormick 2012) of ionocyte. The model of Laurent et al. (1995) seems to match, at least in part, the Type IV "seawater ionocyte", which is thought to result from a transformation of the Type III ionocyte seen in freshwater and dilute salinities (Hiroi et al. 2005; Hiroi and McCormick 2012; Dymowska et al. 2012; Inokuchi et al. 2022).

In the present IHC study on the gills of the Magadi tilapia, we have applied a battery of antibodies that has proven useful in characterizing the various ionocytes in other teleosts. Our first goal was to determine whether the ionocytes fit into the three or four categories identified in other tilapine fishes (Dymowska et al. 2012; Hiroi et al. 2012; Inokuchi et al. 2022). A second objective was to evaluate the transport model of Laurent et al. (1995) for the most abundant type of ionocyte, and a third was to confirm the tentative localization of the mtUT urea transporter to the pavement cells (Walsh et al. 2001).

Materials and methods

Animals

Adult *O.A. grahami* (2–5 g) were collected by seine net from Fish Springs Lagoon (1° 53′ 30.2″S, 36° 18′ 09.9″E) at the edge of Lake Magadi, Kenya. The water chemistry of Fish Spring Lagoon measured at the time of capture is presented in Supplementary Table S1.

Collections were carried out under permission from the Department of Fisheries, Ministry of Livestock and Fisheries (Kenya), and the Magadi Soda Foundation. The research complied with the laws of Kenya, and was performed under a research ethics clearance permit (NCST/RR1/12/1/MAS/99) from the National Commission for Science, Technology and Innovation (NACOSTI Kenya), under a research permit issued by the National Council for Science and Technology of the Ministry of Higher Education, Science, and Technology of the Republic of Kenya. Protocols were approved by the Animal Use and Ethics Committee of the Faculty of Veterinary Medicine, University of Nairobi.

Fish were euthanized with an overdose of MS-222 (Syndel, Nanaimo, BC, Canada), wrapped in aluminum foil, and flash-frozen whole in liquid nitrogen, then transported at − 80 °C in a dry shipper (CX100, Taylor Wharton, Columbus, OH, USA), and stored in an ultracold freezer at − 80 °C for later processing.

Histology and immunohistochemistry

Whole frozen fish were immersion-fixed in Dent's fixative (20%DMSO/methanol) chilled to − 80 °C. After 1 week the solution was substituted with 100% methanol at − 80 °C and then slowly brought to 4 °C over 3 days. Whole fish were then decapitated and the heads divided medially. After bringing the samples to room temperature, they were cleared with xylene, infiltrated with Type 6 paraffin (Richard-Allen Scientific, San Diego, CA, USA) and embedded for sectioning.

Five-micrometer sections were collected onto either plain or APS (3-aminopropyl triethoxy silane) coated slides for respective histological staining with Periodic Acid Schiffs (PAS) and Alcian blue (pH 2.5) staining, or immunohistochemical staining for ion transporter proteins according to Wilson et al. (2007). Immunohistochemistry was performed with combinations of antibodies that included mouse monoclonal cystic fibrosis transmembrane regulator (CFTR), Na^+/K^+-ATPase (NKA) α subunit, and Na^+: K^+: 2 Cl^- co-transporter-1/Na^+: Cl^- co-transporter (NKCC1/NCC) antibodies plus rabbit polyclonal NKA, Na^+: HCO_3^- co-transporter (NBCe1), urea transporter [toadfish (tf) UT], the vacuolar type proton pump (VHA) B subunit, and NHE3b antibodies. See Table 1 for specific details on the antibodies and Fig S1 for alignments of the antigenic peptide and target amino acid sequences of NBCe1, NHE3b and UT. All three targets show high identity. NBCel, tfUT and NHE3b antibodies were kindly provided by Drs. S. Hirose (Tokyo Institute of Technology, Yokohama, Japan), P. Walsh (U. Ottawa, Ottawa, Canada), and J. Hiroi (St. Marianna University School of Medicine, Kawasaki, Japan), respectively. Secondary antibodies used were goat anti-mouse Alexa 594 and goat anti-rabbit Alexa 488 conjugated antibodies (Thermo Fisher Scientific, Toronto, ON, Canada) diluted 1:500. Negative and null controls were performed, which consisted of primary antibody substitution with either normal rabbit serum or antibody dilution buffer, respectively. When possible, antigen pre-absorption controls were also performed. For monoclonal antibody negative controls, equivalently diluted isotyped culture supernatant was used. In these experiments,

Table 1 List of antibodies used to probe *Oreochromis (Alcalicus) grahami* gill sections. The antibody name, target, dilution in 1% Bovine Serum Albumin/Phosphate Buffered Saline with 0.05% Tween-20 and 1% Normal Goat Serum for Immunohistochemistry (IHC) or 5% blotto in Tris Buffered Saline with 0.05% Tween-20 for Western blotting (WB), host species, predicted molecular mass (kDa) and reference information

Antibody	Target	IHC	WB	Host spp.	Predicted molecular mass	Ref
α5	NKA α subunit	1:100	1:500	Mo	100	Takeyasu et al. 1988
αR1	NKA α subunit VTGVEEGRLIFDNLKKC	1:500	1:500	Rb	100	Ura et al. 1996; Wilson et al. 2007
T4	NKCC/NCC human NKCC1 C-terminus (Met902-Ser1212)	1:100	1:1000	Mo	115/112	Lytle et al. 1995 Hiroi et al. 2008
673**	Mefugu *T. obscurus* mfNBCe1 [amino acid (aa) residues 985–1075]	1:100	1:1000	Rb	119	Kurita et al. 2008
VHA B	RKDHADVSNQLYACYA	1:500	1:1000	Rb	56	Wilson et al. 2007; Wood et al. 2013
NHE3b**	Trout Nhe3b position 755–769: GDEDFEFSEGDSASG; 818–839: PSQRAQLRLPWTPSNLR-RLAPL	1:200		Rb	95	Wright et al. 2016
24–1	CFTR c-term	1:200	n/a	Mo	160	R&D systems Marshall et al. 2002
tfUT-A** Slc14a2	YNNHFPQVLIQPRSELP aa 198–214	1:200	1:1000	Rb	53*	Bucking et al. 2013
tfUT-B** Slc14a2	SEIDLPKLFMSIPV aa219-232	1:200	1:1000	Rb	53*	Bucking et al. 2013

*Note that the UT peptides are highly hydrophobic and their migration in SDS-PAGE deviates from the molecular mass predicted from the amino acid sequence. For example rat UT-A1 is 929 aa with a predicted MW of 102 kDa (expasy MW tool) and yet the core protein migrates at 88 kDa (Bradford et al. 2001). UT-A1 is highly hydrophobic membrane protein and migrates faster than predicted. Magadi UT has a predicted MW 53 kDa

**See Figure S1 for antigenic peptide alignments with tilapia predicted amino acid sequences

the clone J3, which is specific for shark NKCC (Slc12a1) was used. Sections were counter-stained with DAPI (4′, 6-diamidine-2′-phenylindole dihydrochloride) and a differential interference contrast (DIC) image collected along with fluorescence using a Leica DM6000B wide-field photomicroscope with a DFX340 camera and LAS IF software (Leica Microsystems GmbH, Wetzlar, Germany). Images were assembled and enhanced (Photoshop CS3, Adobe San Jose, CA, USA) while maintaining the integrity of the data.

The distribution of NKA immunoreactive ionocytes was determined in 35 randomly selected gill filaments in transverse section. Filaments were divided into five equal regions (1–5) from the efferent (leading) edge to the afferent (trailing) edge of the cross sections and NKA-IR cells counted manually and expressed per μm linear distance of filament width. Data were analysed by a Kruskal–Wallis one-way ANOVA followed by a Tukey's test ($p < 0.05$). In addition, a total of 250 cells were analyzed for size (μm^2), shape (shape factor), density (# cells/mm) and percentage of Type II (apical NCC), Type IV (basolateral NKCC1) and Type I (no NKCC/NCC) ionocytes in sections of the trailing edge region of 10 gill filaments based on T4 immunoreactivity of NKA immunopositive cells using SigmaScan Pro image analysis software (v.5, SPSS). For shape factor (0 to 1) a value of 1 indicates a perfect circle.

Western blotting

Gill sample preparation, SDS polyacrylamide gel electrophoresis (10%T) and Western blotting were performed as described in Wood et al. (2013) and Wilson et al. (2007). Crude gill homogenate was separated using a BioRad mini-PROTEAN 3 system with prep-gel comb and semi-dry transfer system. The PVDF membrane was blocked with 5% blotto in Tris Buffered Saline with 0.05% Tween-20 and probed using a BioRad mini- PROTEAN 2 multiscreen apparatus. See Table 1 for the dilutions of primary antibodies used. Secondary antibodies were conjugated to horse radish peroxidase. Bands were detected using enhanced chemiluminescence and documented using a FuijFilm LAS4000mini imager.

Results

Tissue morphology

Flash freezing whole fish in liquid nitrogen, storage at − 80 °C and fixation in Dent's fixative at low temperature (− 80 °C) resulted in tissue sections of reasonable quality for histological analysis (Fig. 1). Gill lamellae were largely devoid

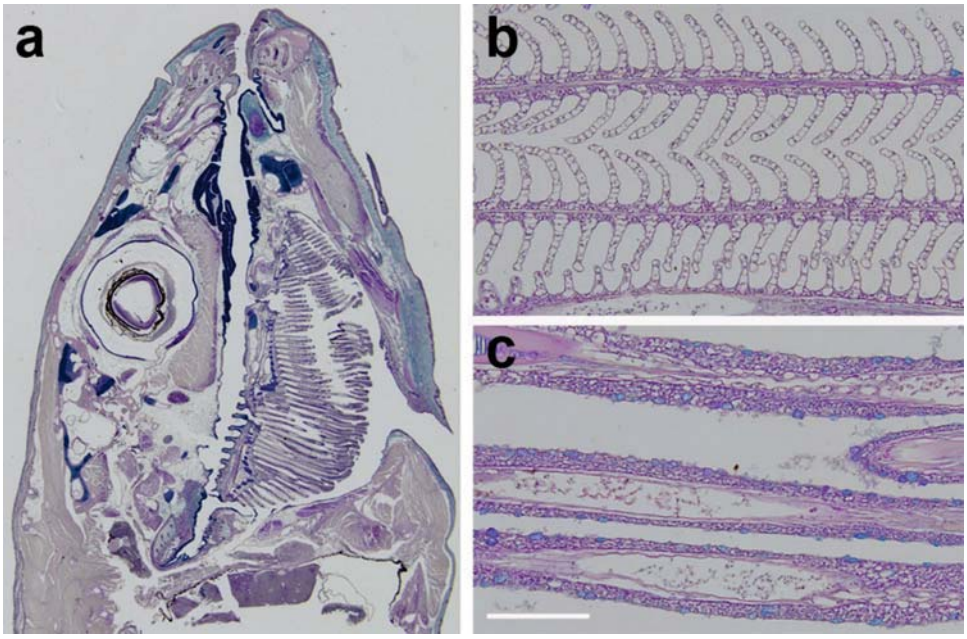


Fig. 1 **a** Sagital section through the head of *O.A. grahami* stained with PAS and Alcian Blue (pH 2.5). Higher magnification regions of sagital sections through the gill filaments revealing **b** lamellae and **c** the trailing edge. Scale bar **a** 0.5 cm or **b**, **c** 100 µm

of large ionocytes which were limited to the gill filament along with large Alcian-blue staining goblet cells. There were some areas where freezing artefact could be identified and thus avoided for analysis.

IHC

On the basis of NKA α-subunit immunoreactivity using either the α5 mouse monoclonal or αR1 rabbit polyclonal antibodies, ionocytes could be easily recognized in the

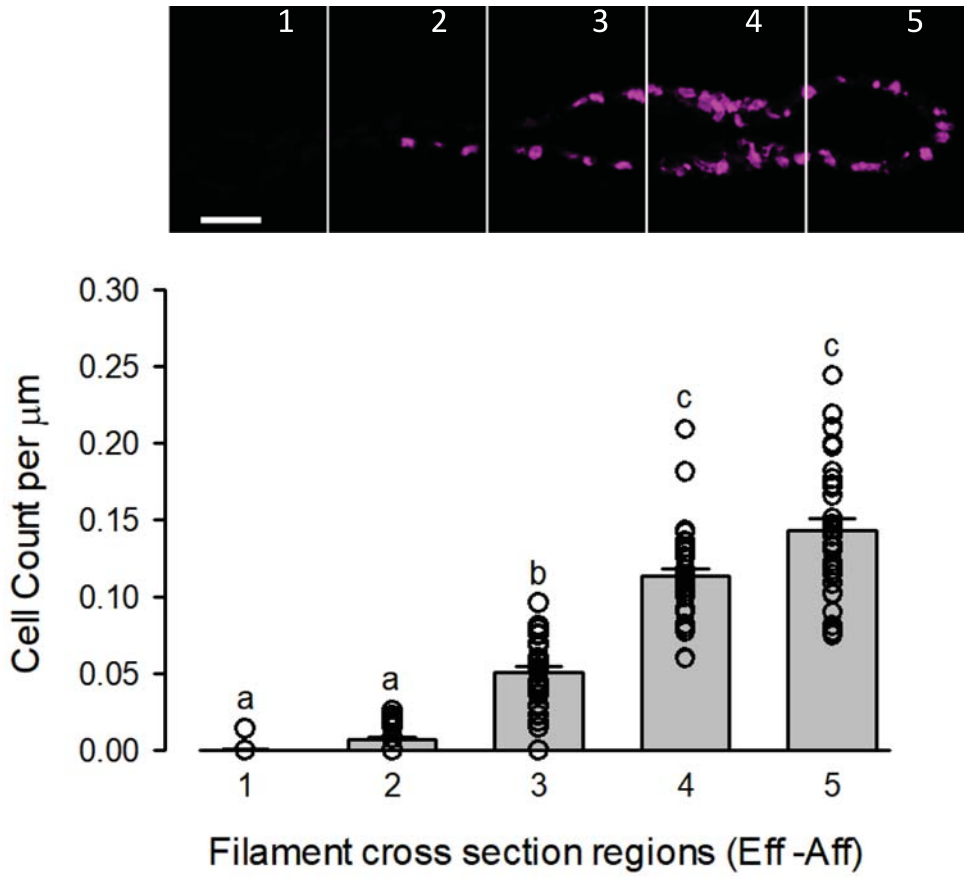


Fig. 2 Distribution of Na^+/K^+-ATPase immunoreactive cells (magenta) from the efferent (1) to afferent (5) side of the gill filament in Magadi tilapia. In total 35 gill filaments transverse sections were analysis. Filaments were divided into five equal regions (1–5) and NKA-IR cells counted and expressed per µm linear distance of filament width. Data were analyzed by a Kruskal–Wallis one way ANOVA followed by a Tukey's test ($p < 0.05$). Bars not sharing like characters are significantly different from each other. A representative gill filament section in shown. Scale bar = 50 µm

filament epithelium of the gills of Magadi tilapia with a dramatic increase in frequency towards the downstream or afferent edge (Figs. 2, 3, 4). These cells were readily identifiable by their apparent cytoplasmic staining which is indicative of the tubular system associated with the basolateral membrane in teleost ionocytes. Two types of ionocytes could be further characterized based on the strength of their NKA immunoreactivity and morphology. Ionocytes with strong NKA immunoreactivity were typically columnar-cuboidal in shape with a less pronounced apical crypt (indentation). In contrast, ionocytes with weaker NKA immunoreactivity were characteristically ovoid-squamous in shape with a prominent apical crypt. These cells could be distinguished from pavement cells that were much more flattened and devoid of detectable NKA immunoreactivity. The NKA immunoreactive ionocytes were further characterized based on expression of other transporters including NKCC, NCC, CFTR, and NBC.

Localization of both the NKCC1 and NCC was done using the T4 mouse monoclonal antibody which recognizes both transporters although they can be differentiated based on subcellular localization (Hiroi et al. 2008). NKCC1 is identified by its basolateral localization similar in appearance to NKA. Weak NKCC1 immunoreactivity was found to co-localize with intense NKA immunoreactivity in the columnar-cuboidal ionocytes corresponding to the type IV subpopulation (Fig. 3). In sections of the flat trailing edge region of gill filaments the type IV ionocytes had an average size of 13.6 μm^2 and shape factor of 0.62 (Fig. 5). In contrast, NCC immunoreactivity was identified on the basis of an apical localization to type II ionocytes. Strong NCC

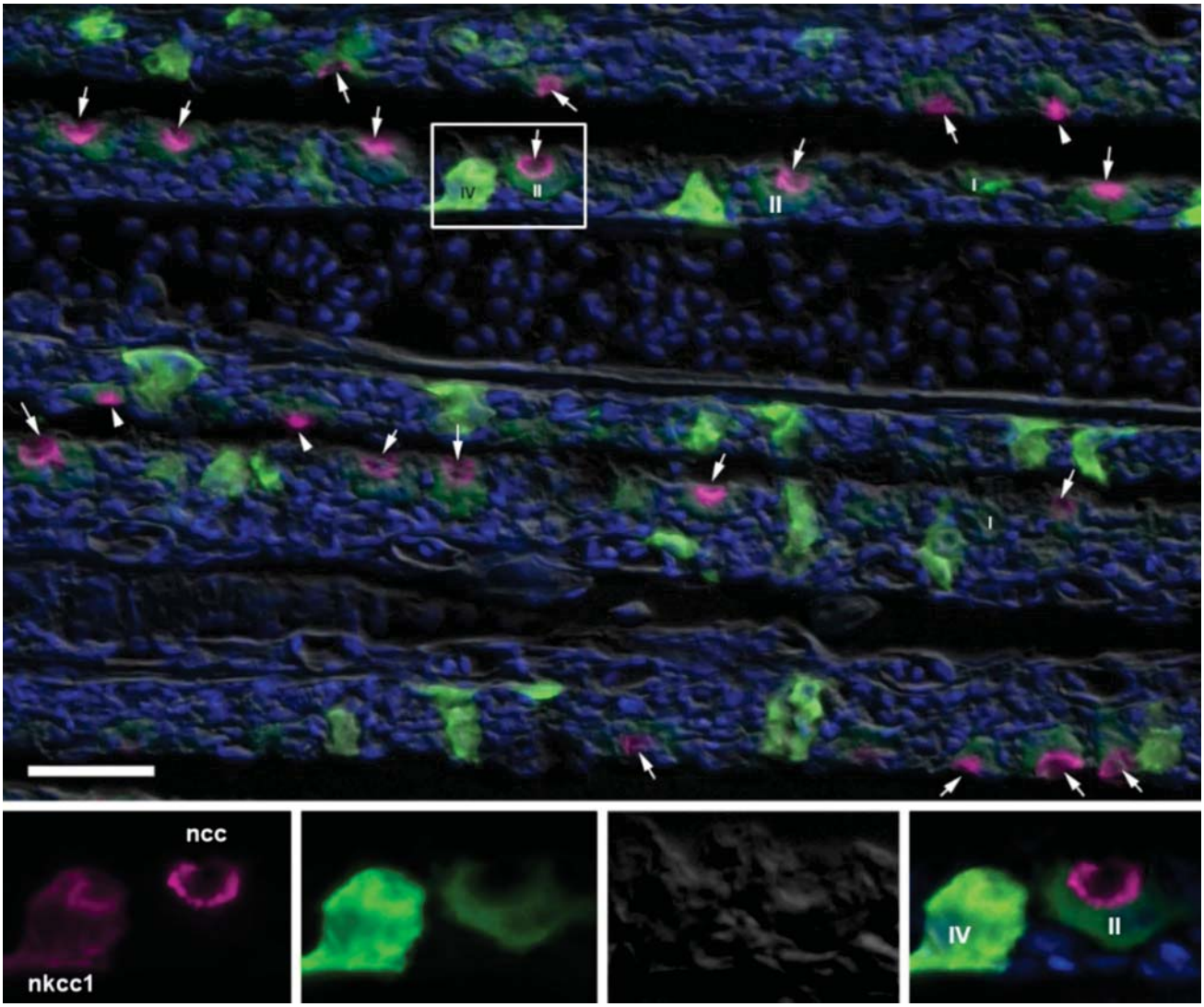


Fig. 3 Double immunofluorescent labeling of NKCC/NCC (magenta; T4 monoclonal antibody) and NKA α subunit (green; rabbit polyclonal) in the trailing edge of the gills of *O.A. grahami*.). Sections are counter stained with DAPI (blue) and overlaid with the DIC image. Inset at 2 × magnification. Scale bar 50 µm

immunoreactivity was present in either a shallow or deeper C-shaped concave crypt or pit in ovoid-squamous ionocytes which exhibited weak NKA immunoreactivity. NKA immunoreactive cells that did not have T4 staining were classified as Type I ionocytes. The Type II ionocytes were smaller (10.7 μm^2) and rounder (shape factor 0.72) than Type IV cells. The majority of ionocytes were type II (60%), while 36% were type IV and the remaining 4% had no T4 immunoreactivity (Type I).

CFTR immunoreactivity was found apically in the columnar-cuboidal type IV ionocytes with strong NKA immunoreactivity (Fig. 4). The apical CFTR staining was restricted to a relatively small apical area in contrast to NCC and did not form a deep crypt or pit. CFTR immunoreactivity was not seen in the ovoid-squamous ionocytes with weak NKA immunoreactivity. The NBCe1-like immunoreactivity was found associated with the ovoid-squamous ionocytes with weaker NKA immunoreactivity (Fig. 3) and apical NCC (Fig. 6). We could not find colocalization of NBCe1 and CFTR to the same cell type (Fig. 7). The tfUT immunoreactivity was found in the lamellar epithelium in a punctiform pattern (Fig. 8). Staining was not associated with NKA-immunoreactive cells which were largely localized to the trailing edge of the filament epithelium. No immunoreactivity was found with the antibodies for V-type H^+-ATPase and NHE3b (latter in Fig. 9). However, positive NHE3b cross reactivity was demonstrated in tilapine kidney (Fig. S2; Wright et al. 2014; Takvam et al. 2021) and one of the antigenic peptides used to create the antibody is 100% identical to tilapia NHE3 (Fig S1). Negative control staining of sections done in parallel showed negligible levels of background fluorescence (Fig. 9).

Western blotting

Immunoblotting was used to confirm antibody cross reactivity (Fig. S3). Both NKA antibodies (αR1 and α5) recognized bands in the predicted 100 kDa range. Probing with the T4 antibody (NKCC/NCC) identified some bands in the 150 kDa range but with some stronger lower molecular mass bands. The NBCe1 antibody (673) recognized a band in the 100

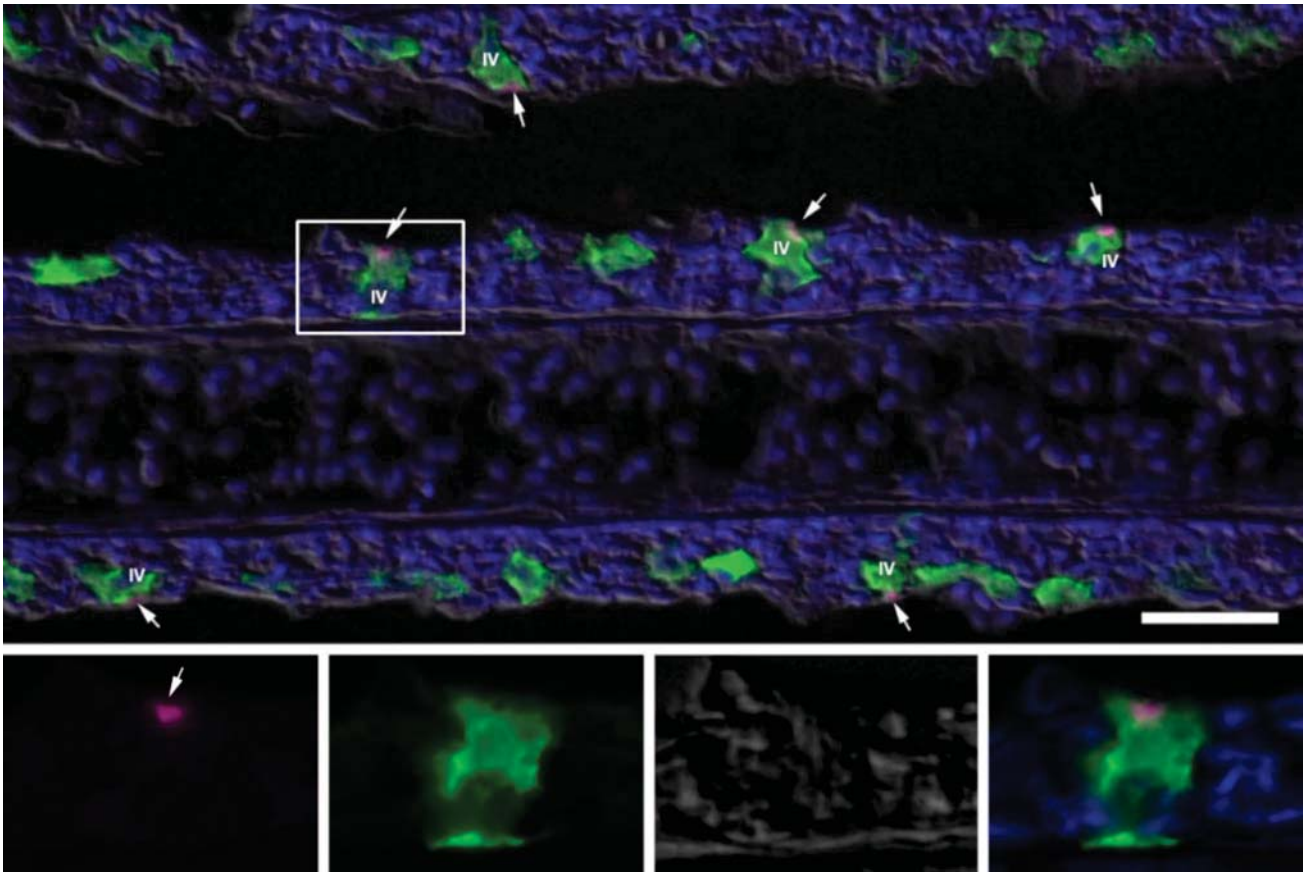


Fig. 4 Longitudinal section through the trailing edge of *O.A. grahami* gill filament double immunolabelled for CFTR (magenta; mouse monoclonal 24–1) and NKA α subunit (green; rabbit polyclonal). See Fig. 3 caption for additional information. Insets are at 2× magnification. Scale bar 50 µm

kDa range. The toadfish UTA antibody recognized a cluster of bands in the 40 kDa range. No bands were detected with either the CFTR or tfUTB antibodies and the unprobed lane.

Discussion

With respect to our original objectives, we have identified three different types of ionocyte in the gills of the Magadi tilapia which fit clearly into three (Types I, II, and IV) of the four categories of ionocytes that have previously been characterized in other tilapine fishes (Hiroi et al. 2005, 2008; Choi et al. 2011; Dymowska et al. 2012; Hiroi and McCormick 2012; Inokuchi et al. 2022). Furthermore, in the second most abundant ionocyte (Type IV), our IHC results have confirmed many elements of the hypothetical model for Na^+ excretion plus base equivalent excretion that was originally proposed by Laurent et al. (1995) on the basis of structure alone. Finally, we have also shown that the facilitated diffusion transporter UT is confined to the pavement cells, and does not occur in ionocytes, confirming the original conclusion of Walsh et al. (2001) that again was based on cell fine structure alone.

Ionocyte types in the gills of *O.A. grahami*

Based on IHC labelling, ionocytes corresponding to Types I, II, and IV of Hiroi et al. (2005), Hiroi et al. (2008), Choi et al. (2011), and Inokuchi et al. (2022) were found in the gills of the Magadi tilapia. This agrees with previous studies using classical techniques that have reported several types of ionocytes in the gills of this species, but without categorization (Maina 1990, 1991; Wood et al. 2002a). The localization of transporters within the ionocyte types is illustrated in Fig. 10.

Type I ionocytes were relatively rare (4% of ionocytes) and stained only for NKA on the basolateral membranes and the tubular network that extends from the base into most of the cytoplasmic region. The antibodies used in the present study did not identify any transporters on the apical membranes. However, there is evidence that in Mozambique tilapia, Type I ionocytes express ROMK (renal outer medullary K^+) channels on their apical membranes and are involved in K^+ excretion (Furukawa et al. 2014). This could be useful in Magadi tilapia which eat mainly blue-green algae such as *Arthrospira* (Coe 1966) that is rich in K^+ (Cogne et al. 2003). Plasma K^+ concentrations (~5 mmol·L^{-1}; Wood et al. 2013) are about twofold environmental concentrations (Supplementary Table S1), and branchial K^+ excretion through ROMK channels would be further aided by the positive TEP inside the fish (Wood et al. 2012). However, since ROMK channels have also been found in Type III and IV cells in Mozambique tilapia (Furukawa et al. 2014; Inokuchi et al. 2022) the more general view is that Type I cells are immature ionocytes with limited or no contact with the outside water, waiting to differentiate into the other types (Inokuchi et al. (2022). There is evidence that *O.A. grahami* can be adapted to dilutions of Lake Magadi down to 1% (Wood et al. 2002a, b) and even to true fresh water (Kavembe et al. 2015), and that other populations in the Magadi basin live naturally in much more concentrated water (see Table 5 in Wilson et al. 2004) than found in Fish Spring Lagoons (Supplementary Table 1), so this capability probably becomes very important under these conditions.

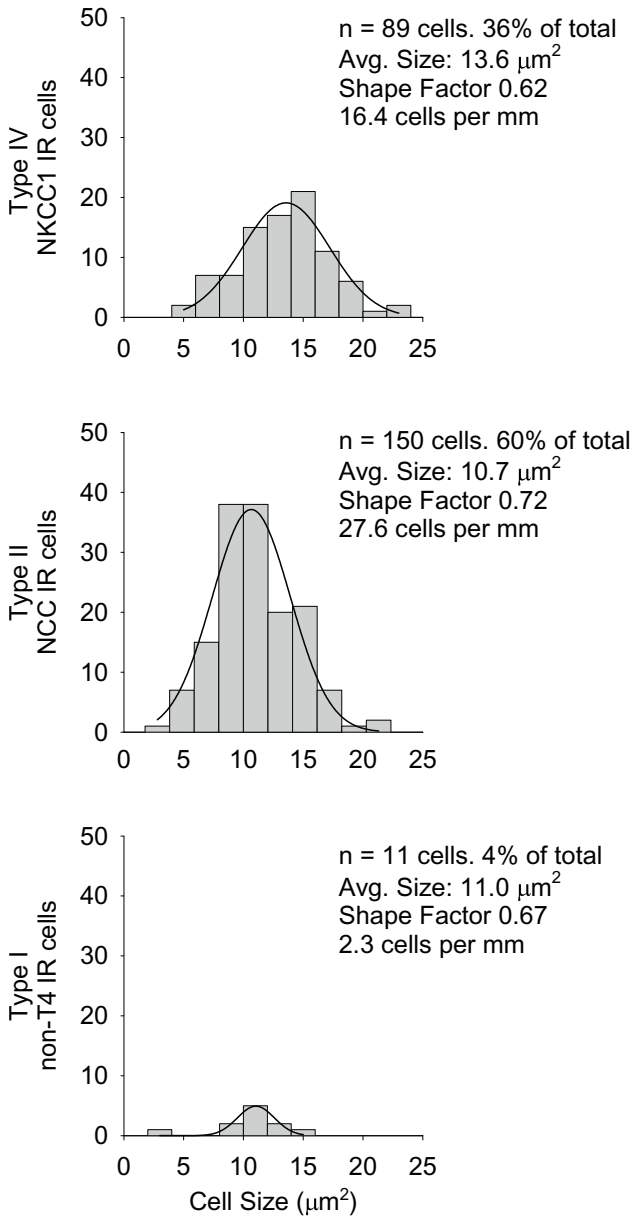


Fig. 5 Analysis of Magadi tilapia branchial ionocytes. The trailing edges of 10 gill filaments double labelled for NKCC/NCC and NKA were analyzed. Type IV (basolateral NKCC1), II (apical NCC) and I (NKA only) cell frequency, shape factor, size and density are calculated. n = 250 cells

Type II ionocytes were identified by apical NCC and basolateral NBCe1 immunoreactivity, and the absence of apical CFTR immunoreactivity (Figs. 3, 6). These combined characteristics were present only in the ovoid-squamous ionocytes which exhibited weak NKA immunoreactivity and pronounced apical pits. They were the most abundant type of ionocyte observed in the gill. Note that according to Choi et al. (2011) and Hiroi and McCormick (2012), the immunoreaction of the T4 antibody used in the present study is attributable to NCC when it appears in the apical membrane, and to NKCC1 when it appears in the basolateral membrane. In other tilapines, the Type II ionocyte is now considered to be a "freshwater ionocyte" responsible for Na^+ and Cl^- uptake from dilute environments, (Hiroi et al. 2005, 2008; Dymowska, et al. 2012; Hiroi and McCormick 2012; Inokuchi et al. 2022). Interestingly, Wood et al. (2002a) reported that ionocytes with this sort of structure increased in abundance when Magadi tilapia were challenged with environmental dilution. Indeed, they became completely dominant when the fish were acclimated to 1% Lake Magadi water. Although not capable of surviving the extreme conditions of Lake Magadi, the transcriptomic analysis of Nile tilapia exposed to alkaline water conditions revealed an increase in gill *slc12a3* (*ncc*) gene expression (Zhao et al. 2020).

In other tilapines, Type II cells decrease at higher salinities, yet they are abundant in *O.A. grahami* in Fish Springs Lagoon where the normal external osmolality is hypertonic and corresponds to about 57% of that of seawater (Supplementary Table S1). The explanation may lie in the unusual ionic composition of Lake Magadi water. In contrast to 57% seawater, Magadi water exhibits a relatively low Cl^- concentration (Supplementary Table S1), much below that of the blood plasma. Indeed, taking the positive TEP inside into account, there is still an electrochemical gradient favouring the outward diffusion of Cl^- at the gills (Wood et al. 2012). To satisfy the need for acquisition of this essential ion, the Magadi tilapia must use the secondarily active uptake of Cl^- via the NCC co-transporters on the Type II ionocytes. The additional (counter-productive) uptake of Na^+ is an unavoidable consequence, which is exported to the internal environment by the basolateral NKA. In this species, we found no IHC evidence for either an apical Na^+/H^+ exchanger or V-type H^+-ATPase, the transporters

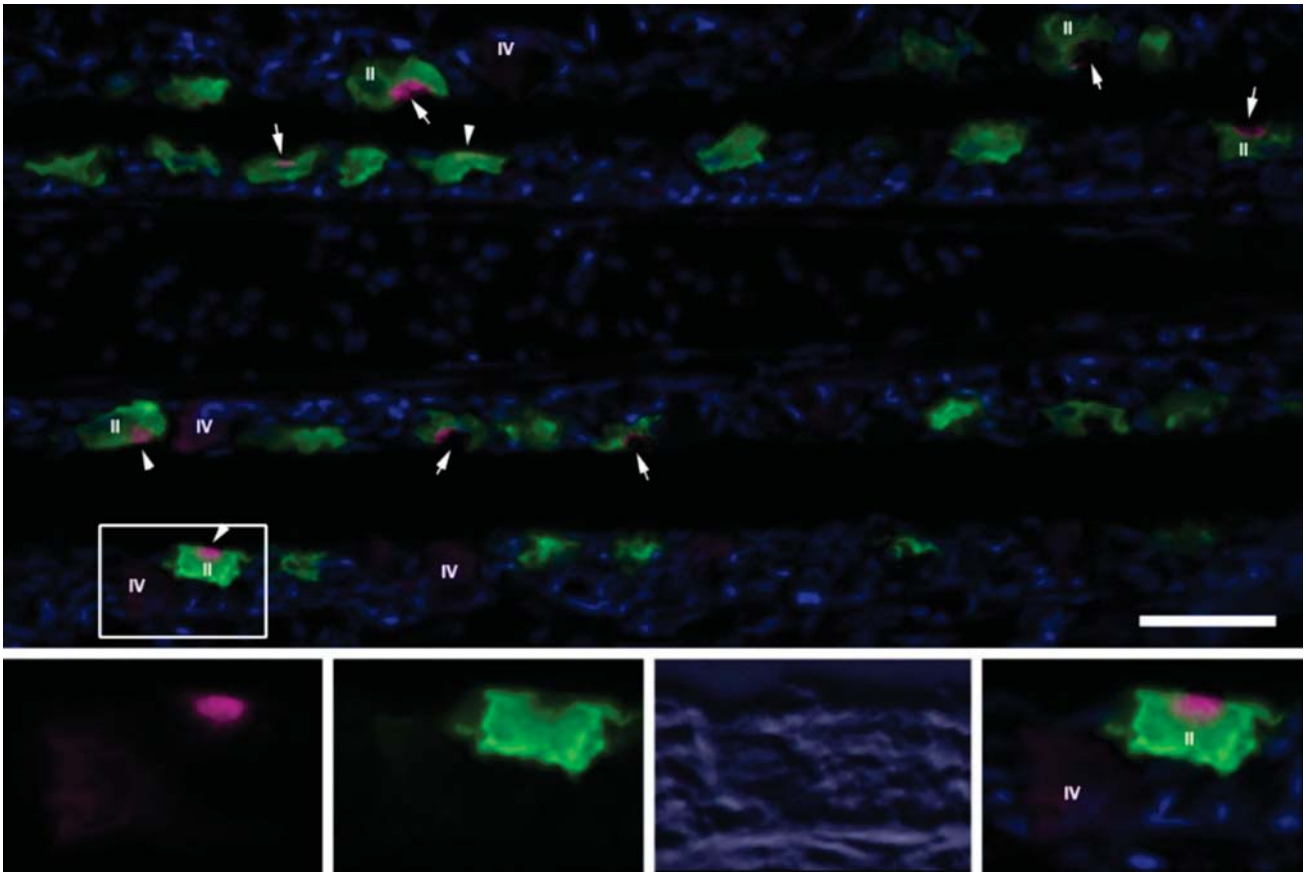


Fig. 6 Double immunofluorescent labeling of NKCC/NCC (magenta; T4 monoclonal antibody) and NBCe1 (green; rabbit polyclonal) in the trailing edge of the gills of O.A. grahami. See Fig. 3 caption for additional information. Inset at 2× magnification. Scale bar 50 µm

usually associated with the active uptake of Na^+ and acid equivalent excretion in the ionocytes of other non-tilapine teleosts (Evans et al. 2005; Dymowska et al. 2012). This is not surprising, as their function would presumably be maladaptive for Na^+ and acid–base homeostasis in the Magadi tilapia. Only NHE3 (and not V-type H^+-ATPase) has been found in other tilapines, and only in Type III and IV ionocytes (Inokuchi et al. 2008; Watanabe et al. (2008); Choi et al. 2011). Type III ionocytes do not appear to be present in *O.A. grahami* although negative immunohistochemical results should be interpreted with some caution.

Type IV cells were the second most abundant ionocyte in the gills of *O.A. grahami* and were recognized by strong NKA immunoreactivity throughout the tubular network of the cytoplasm and along the basolateral membrane, coupled with strong apical expression of CFTR, and relatively weak expression of NKCC1 which followed the same pattern as that of NKA (Figs. 3, 6, 7). These characteristics were confined to the columnar-cuboidal ionocytes with less prominent apical pits. These cells clearly resemble the ionocytes that are dominant in other tilapines when acclimated to seawater (Hiroi and McCormick 2012; Inokuchi et al. 2022). Note that when other tilapines are transferred from less saline to more saline waters, Type IV ionocytes may be generated by the transformation of Type III ionocytes, as well as by the differentiation of Type I ionocytes (Choi et al. 2011). However, Type III ionocytes, which would have been identified by the presence of apical NHE and absence of apical CFTR, were not seen in the present study. The Type IV ionocytes identified in the present study appear to correspond to the most abundant ionocytes that were described in Magadi tilapia on the basis of morphology alone by Maina (1990), Maina (1991), Laurent et al. (1995) and Wood et al. (2002a). However, our IHC results indicate that the majority of ionocytes in the gill filament trailing edge are Type II (60% versus 36% Type IV). Laurent et al. (1995) (see Fig. 5) also documented that they were bordered by accessory cells that play an important role in the model for NaCl excretion (Silva et al. 1977; Hiroi and McCormick 2012) in seawater teleosts.

Evaluation of the Laurent model for ion transport in Type IV ionocytes of *O.A. grahami*

Very clearly, the model proposed by Laurent and co-workers (1995) for Na^+, Cl^-, and base equivalent transport across the gills of the Magadi tilapia was prescient. The first support for this

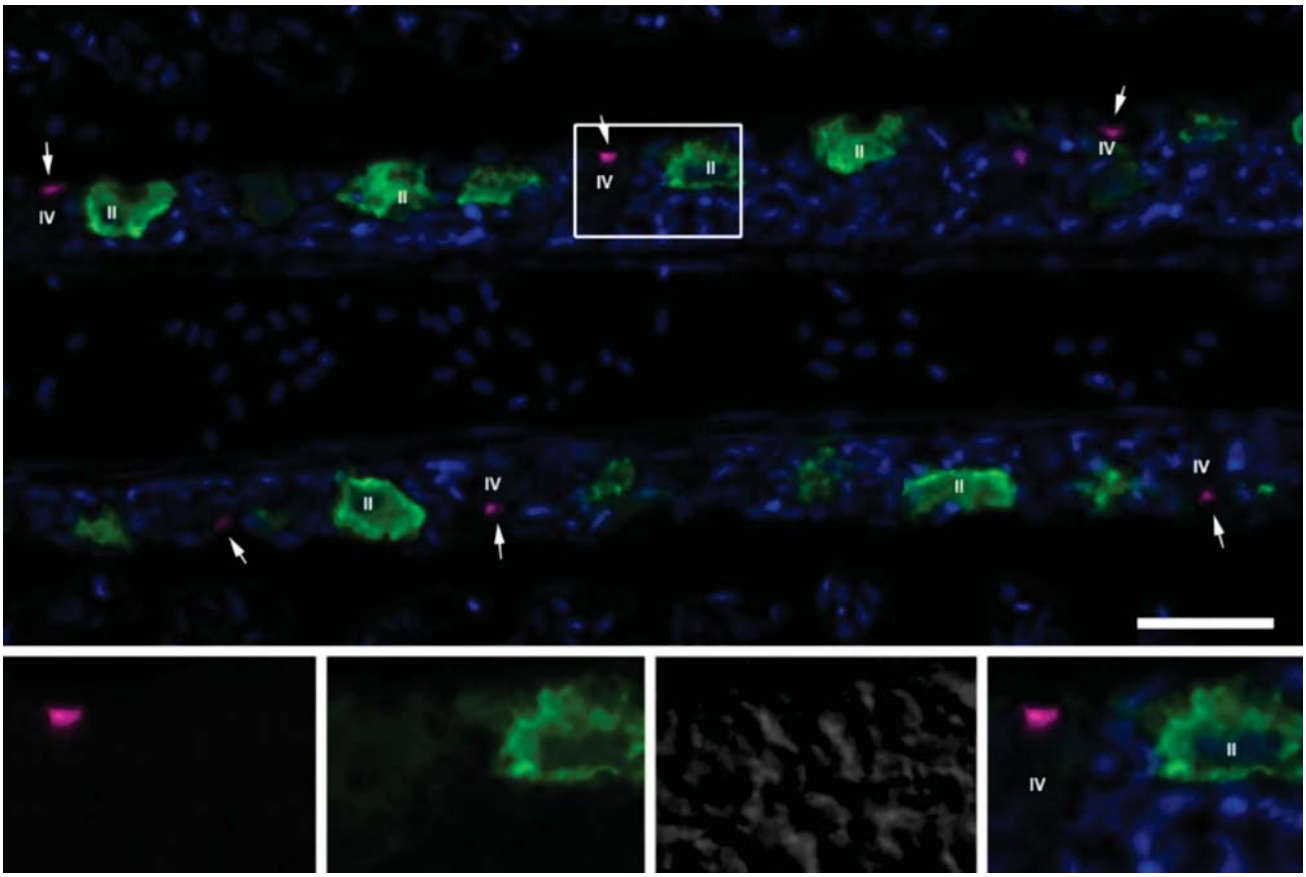


Fig. 7 Longitudinal section through the trailing side of the Magadi tilapia gill filament double labelled for both CFTR (magenta) and NBCe1 (green). See Fig. 3 caption for additional information. Inset at 2× magnification. Scale bar 50 µm or 25 µm for the insets

model was provided by electrophysiological data showing that there is an inside positive TEP of partially electrogenic origin that is responsive in the expected fashion to experimental manipulations of HCO_3^- gradients (Wood et al. 2012). The present IHC data provide additional support for the presence of key elements in the Type IV ionocytes of Magadi tilapia, namely apical CFTR and basolateral NKCC1, powered by basolateral NKA.

As noted in the Introduction, Laurent's scheme was a modification of the classic "chloride cell" model of Silva et al. (1977), with base equivalents replacing Cl^- at every step. In 1995, the anion channel for apical exit of Cl^- in fish ionocytes had not been characterized, and it was not until three years later that it was tentatively identified as CFTR (Singer et al. 1998), a concept that is now generally accepted (Marshall and Singer 2002; Evans et al. 2005; Hiroi and McCormick 2012). Laurent proposed that this unknown apical anion channel could serve as the exit pathway for base equivalents, but it was only around that same time that the first evidence was emerging from mammalian studies that CFTR could also conduct HCO_3^- (Poulsen et al. 1994; Linsdell et al. 1997; Tang et al. 2009; Ishiguro et al. 2009; Bridges 2012). In spotted sea bass (*Lateolabrax maculatus*) acclimated to alkaline conditions increased branchial *cftr* gene expression (Zhang et al. 2026). Laurent also proposed that a basolateral NKCC-like transporter, energized by basolateral NKA, could serve as the entry pathway for base equivalents, together with Na^+, into the ionocyte. Na^+ would be exported by NKA into the paracellular channels for exit into the external water through leaky junctions between the ionocytes and accessory cells. This export of Na^+ would create the electrochemical gradient for the operation of the NKCC-like transporter. NKA is highly abundant and NKCC1 is present in the basolateral membranes of Type IV ionocytes (Figs. 4, 7), and accessory cells are also present, in accord with the Laurent model. However, we are aware of no evidence whether or not NKCC can transport base equivalents such as HCO_3^- and CO_3^{2-} on its anion binding site, so further research is necessary to evaluate this idea. Certainly, basolateral NBC is not present in Type IV ionocytes (Fig. 7), which tends to eliminate this alternate pathway for HCO_3^- entry.

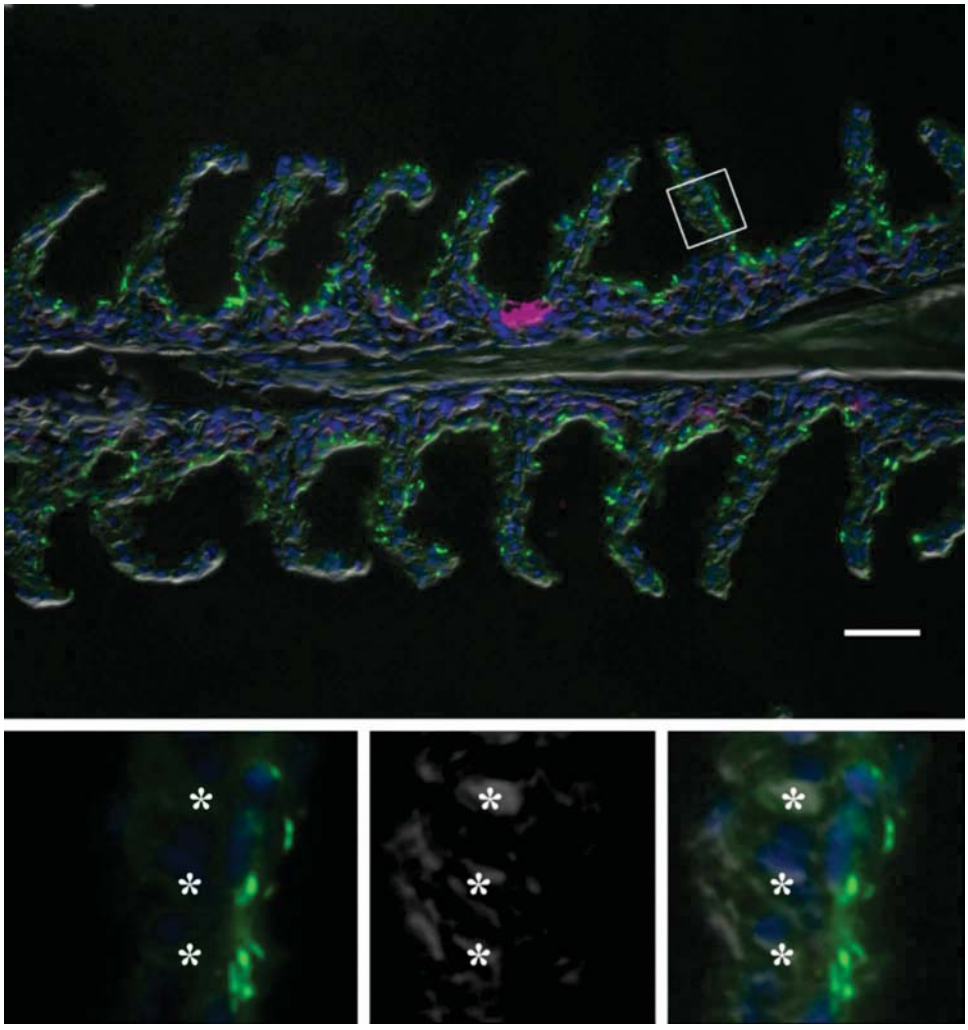


Fig. 8 Immunohistochemical localization of the urea transporter (UT; green) double labelled with the NKA (magenta) in cryosections of the gills of the Magadi tilapia. Sections are counter stained with DAPI (blue) and overlaid with the DIC image. Insets are at 5× magnification. The asterisks indicate red blood cells at the centre of the lamellae. Scale bar 100 µm

Finally, Laurent proposed that an apical Cl^-/HCO_3^- exchanger could account for Cl^- uptake from the water. There is no IHC evidence for or against this idea in the present study or in previous work on other tilapine fishes. However, as argued earlier, the presence of apical NCC on Type II ionocytes (Figs. 3, 6) may provide the pathway needed for Cl^- uptake from the external water.

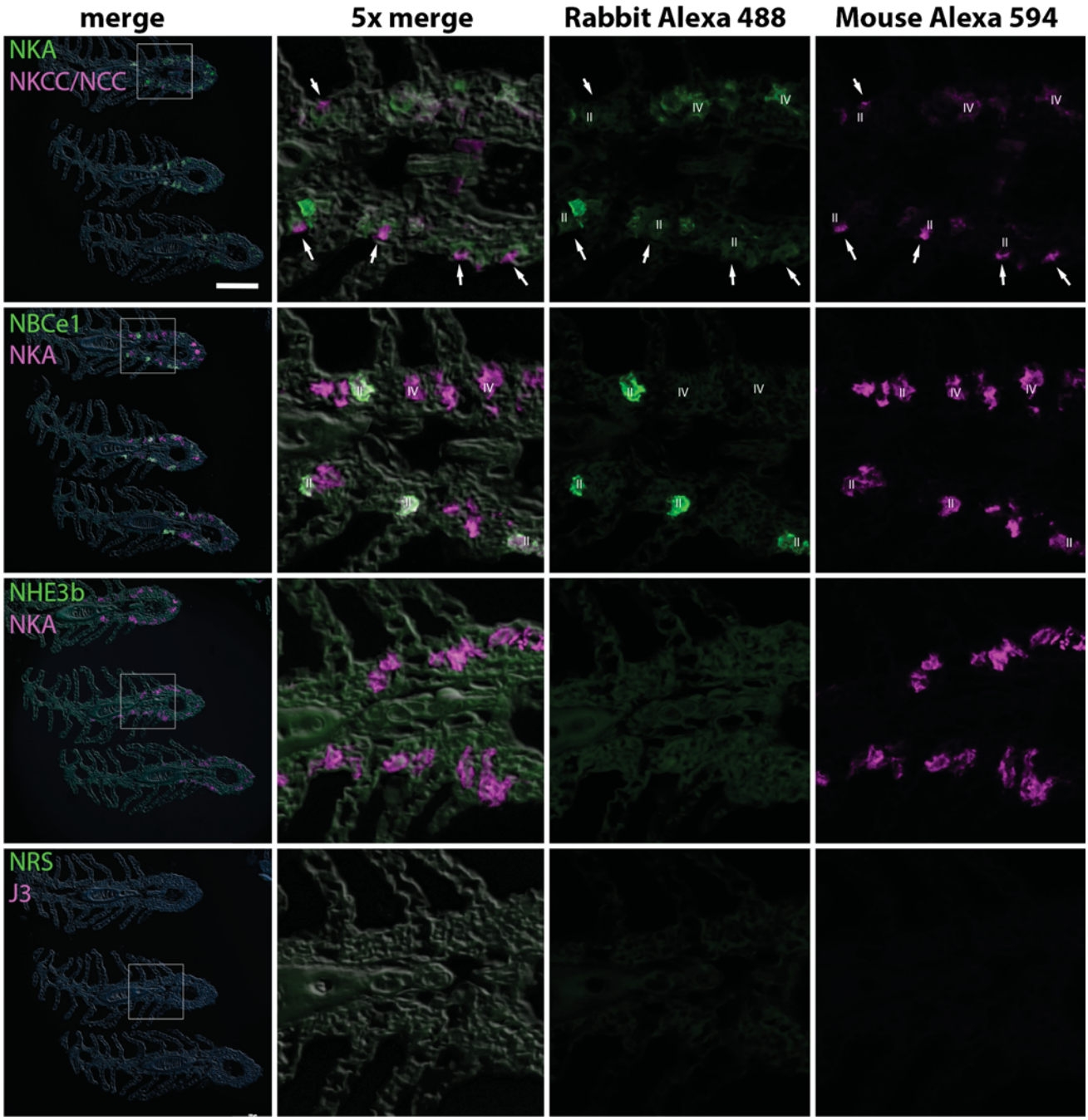


Fig. 9 Immunofluorescence staining of Magadi tilapia gill filaments in sagittal section (left to right efferent to afferent orientation). Merged images are overlaid with the DIC images to show tissue structures. Sections were double stained for Na^+/K^+-ATPase (NKA; rabbit polyclonal aR1) with $Na^+:K^+:2Cl^-$ cotransporter/ $Na^+:Cl^-$ cotransporter (NKCC/NCC, mouse T4 monoclonal), and either $Na^+:HCO_3^-$ cotransporter e1 (NBCe1, rabbit polyclonal), or Na^+/H^+ exchanger 3b (NHE3b, rabbit polyclonal) with NKA (mouse α5 monoclonal). Negative control staining was performed with Normal Rabbit Serum (NRS) and isotyped mouse monoclonal J3. Ionocyte subtypes II and IV are indicated. Scale bar 100 µm

Localization of UT exclusively to the pavement cells in the gills of *O.A. grahami*

The fully ureotelic *O.A. graham* was only the second teleost species in which a UT-type facilitated diffusion transporter was cloned from the gills and characterized (Walsh et al. 2001). The initial discovery was in the facultatively ureogenic gulf toadfish (*Opsanus beta*) (Walsh et al. 2000). However, we now know that UTs are expressed in the gills of many teleosts, even though most are ammoniotelic (LeMoine and Walsh 2015). In the Magadi tilapia, the presence of intense vesicular trafficking in the pavement cells, and its absence in the pavement cells of the closely related Nile tilapia, led to the tentative conclusion that the UTs were expressed in the pavement cells (Walsh et al. 2001). The present IHC observations confirm this conclusion, showing no UT in NKA-immunoreactive cells on the filament, but clear staining in pavement cells in the lamellar epithelium (Fig. 8). In this regard, the pattern is similar to the UT expression seen only in the pavement cells of the ammoniotelic plainfin midshipman (*Porichthys notatus*) (Bucking et al. 2013) but differs from that in its close relative, the ureogenic gulf toadfish, where UT expression is localized to NKA immunoreactive cells on the filament (Bucking et al. 2013). Similarly, in the ammoniotelic eel, UT is seen only within NKA-immunoreactive cells on the filament, and not in pavement cells (Mistry et al. 2001). Clearly, patterns vary amongst species, regardless of ureotelism versus ammoniotelism. However, as illustrated by Walsh et al. (2001), urea excretion rates in the 100% ureotelic Magadi tilapia are so much higher than in other fish that the much greater surface area of the pavement cells relative to the ionocytes may be required for efficient clearance.

Future directions

The current IHC data show that the Magadi tilapia has three of the four basic ionocyte types that have been characterized in the gills of other tilapines and suggest that they have been subtly re-engineered so as to function in such an unusual water chemistry. However, antibodies can reliably identify only proteins against which they are made. The recent full sequencing of the genome in this species (Bernardi et al. 2024) opens up the possibility to look for many more transport proteins in the gills, both by IHC and in situ hybridization. Another powerful avenue for future research is to employ the opercular epithelium of the Magadi tilapia, which is rich in ionocytes (Laurent et al. 1995), as a flat gill surrogate in vitro. Both classical (e.g., Ussing chamber; McCormick et al. 1992) and modern techniques (e.g., scanning ion-selective electrode technique or SIET; Horng et al. 2009) that have been successfully used on comparable preparations from other tilapines can then be employed to mechanistically characterize the ion transport mechanisms that allow this unique fish to live in such a hostile environment.

Dedication

We dedicate this paper to the memory of our friend, mentor, and co-author Pierre Laurent who participated in three scientific expeditions to Lake Magadi, and taught us much about gills and about life.

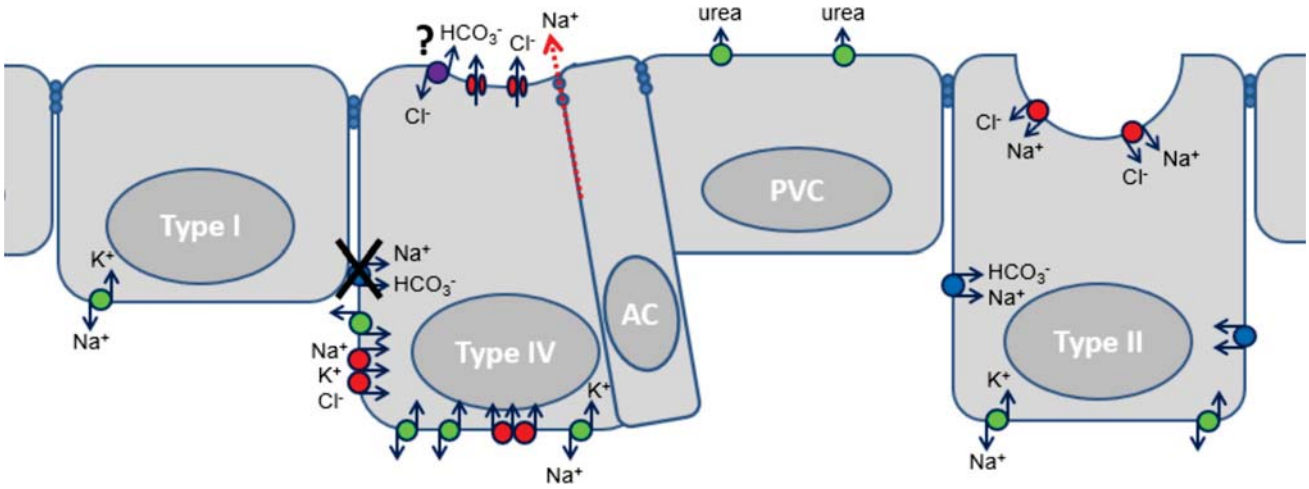


Fig. 10 Summary figure of gill ion transporter expression patterns. Basolateral NKA (green) colocalizes with NKCC1 (red) in seawater (sw) type ionocyte. CFTR anion channels (red) are expressed apically in the cells, and we propose an apical AE (purple) is also present. Basolateral NBC (blue) was not found in these cells. A second freshwater (fw) type ionocyte with basolateral NKA and NBC and apical NKCC/NCC is also present. Based on evidence in *O. mossabicus*, this is likely NCC rather than NKCC2. Urea transporter (UT, green) was observed apically in pavement cells (PVCs)

Supplementary Information The online version contains supplementary material available at https://doi.org/10.1007/s00441-026-04081-6.

Acknowledgements We thank the Magadi Soda Company, in particular John Ndonga and John Kabera, for their cooperation, Dishon Muthee and George Muthee furnished invaluable assistance in the field, and the University of Nairobi for logistic support.

Author contributions J.M.W and C.M.W wrote the main manuscript text. J.M.W, C.M.W., P.L. and C.C. made substantial contributions to the conception of the work; J.M.W. and P.G.F. performed immunohistochemical work; H.L.B., A.B., L.F.B., J.N.M., O.E.J., L.F.B., G.D.K., M.B.P. and R.O.O. collected material and performed some of the experiments; R.O.O. organized the field campaign; all authors contributed to the execution and interpretation of the study, and to drafting and revising the article.

Funding CMW was supported by the Canada Research Chair Program. AB is a Research Fellow from the Conselho Nacional de Desenvolvimento Científico e Tecnológico (CNPq, Brazil) and was supported by the International Canada Research Chair Program from the International Development Research Centre (IDRC, Ottawa, Canada). Funded by Natural Sciences and Engineering Research Council of Canada (NSERC) Discovery grants to CMW (RGPIN-2017–03843, RGPIN-2023–03714) and JW (RGPIN-2019–06838), a grant from the Brazilian CNPq to AB, and a grant from the National Research Foundation of South Africa to JM.

Data availability All data supporting the findings of this study are available within the paper, its Supplementary Information and through FigShare https://doi.org/10.6084/m9.figshare.32325447.

Declarations

Competing interests None

References

Bergman AN, Laurent P, Otiang'a-Owiti G, Bergman HL, Walsh PJ, Wilson P, Wood CM (2003) Physiological adaptations of the gut in the Lake Magadi tilapia, Alcolapia grahami, an alkaline-and saline-adapted teleost fish. Comp Biochem Physiol 136A:701–715

Bernardi G, Kavembe GD, Bergman HL, Bucciarelli G, Wood CM (2024) The genome organization of the Lake Magadi tilapia, *Oreochromis alcolapia grahami*, a cichlid extremophile. J Great Lakes Res 50(3):102326

Bradford AD, Terris JM, Ecelbarger CA, Klein JD, Sands JM, Chou CL, Knepper MA (2001) 97-and 117-kDa forms of collecting duct urea transporter UT-A1 are due to different states of glycosylation. Am J Physiol 281:F133–F143

Bridges RJ (2012) Mechanisms of bicarbonate secretion: lessons from the airways. Cold Spring Harb Perspect Med 2:a015016

Bucking C, Edwards SL, Tickle P, Smith CP, McDonald MD, Walsh PJ (2013) Immunohistochemical localization of urea and ammonia transporters in two confamilial fish species, the ureotelic Gulf toadfish (*Opsanus beta*) and the ammoniotelic plainfin midshipman (*Porichthys notatus*>). Cell Tissue Res 352:623–637

Choi JH, Lee KM, Inokuchi M, Kaneko T (2011) Morphofunctional modifications in gill mitochondria-rich cells of Mozambique tilapia transferred from freshwater to 70% seawater, detected by dual observations of whole-mount immunocytochemistry and scanning electron microscopy. Comp Biochem Physiol A 158:132–142. https://doi.org/10.1016/j.cbpa.2010.09.019

Coe MJ (1966) The biology of *Tilapia grahami* Boulenger in Lake Magadi, Kenya. Acta Trop 23:146–177

Cogne G, Lehmann B, Dussap CG, Gros JB (2003) Uptake of macrominerals and trace elements by the cyanobacterium *Spirulina platensis* (*Arthrospira platensis* PCC 8005) under photoautotrophic conditions: culture medium optimization. Biotechnol Bioeng 81(5):588–593

De Boeck G, Wood CM, Brix KV, Sinha A, Matey V, Johannsson OE, Bianchini A, Bianchini LF, Maina JN, Kavembe GD, Papah MB, Kisipan ML, Ojoo RO (2019) Fasting in the ureotelic Lake Magadi tilapia, Alcolapia grahami, does not reduce its high metabolic demand. Conservation Physiol. https://doi.org/10.1093/conphys/coz060

Dymowska AK, Hwang PP, Goss GG (2012) Structure and function of ionocytes in the freshwater fish gill. Respir Physiol Neurobiol 184(3):282–292

Eddy FB, Maloiy GMO (1984) Ionic content of body fluids and sodium efflux in Oreochromis alcalicus grahami, a fish living at temperatures above 30 °C and in conditions of extreme alkalinity. Comp Biochem Physiol 78A:359–361

Eddy FB, Bamford OS, Maloiy GMO (1981) Na^+ and Cl^- effluxes and ionic regulation in *Tilapia grahami*, a fish living in conditions of extreme alkalinity. J Exp Biol 91:349–353

Evans DH, Piermarini PM, Choe KP (2005) The multifunctional fish gill: dominant site of gas exchange, osmoregulation, acid-base regulation, and excretion of nitrogenous waste. Physiol Rev 85(1):97–177

Ford AG, Bullen TR, Pang L, Genner MJ, Bills R, Flouri T, Ngatunga BP, Rübere L, Schlieweng UK, Seehausen O, Shechonge A, Stiassny MLJ, Turner GF, Day JJ (2019) Molecular phylogeny of Oreochromis (Cichlidae: Oreochromini) reveals mito-nuclear discordance and multiple colonisations of adverse aquatic environments. Mol Phylogenet Evol 136:215–226

Furukawa F, Watanabe S, Kakumura K, Hiroi J, Kaneko T (2014) Gene expression and cellular localization of ROMKs in the gills and kidney of Mozambique tilapia acclimated to fresh water with high potassium concentration. Am J Physiol 307:R1303–R1312

Hiroi J, McCormick SD (2012) New insights into gill ionocyte and ion transporter function in euryhaline and diadromous fish. Respir Physiol Neurobiol 184(3):257–268

Hiroi J, McCormick SD, Ohtani-Kaneko R, Kaneko T (2005) Functional classification of mitochondrion-rich cells in euryhaline Mozambique tilapia (*Oreochromis mossambicus*) embryos, by means of triple immunofluorescence staining for Na^+/K^+-ATPase, $Na^+/K^+/2Cl^-$ cotransporter and CFTR anion channel. J Exp Biol 208:2023–2036. https://doi.org/10.1242/jeb.01611

Hiroi J, Yasumasu S, McCormick SD, Hwang PP, Kaneko T (2008) Evidence for an apical Na–Cl cotransporter involved in ion uptake in a teleost fish. J Exp Biol 211:2584–2599

Horng JL, Hwang PP, Shih TH, Wen ZH, Lin CS, Lin LY (2009) Chloride transport in mitochondrion-rich cells of euryhaline tilapia (*Oreochromis mossambicus*) larvae. Am J Physiol 297(4):C845–C854

Inokuchi M, Hiroi J, Watanabe S, Lee KM, Kaneko T (2008) Gene expression and morphological localization of NHE3, NCC and NKCC1a in branchial mitochondria-rich cells of Mozambique tilapia (*Oreochromis mossambicus*) acclimated to a wide range of salinities. Comp Biochem Physiol A Mol Integr Physiol 151:151–158

Inokuchi M, Hiroi J, Kaneko T (2022) Why can Mozambique tilapia acclimate to both freshwater and seawater? Insights from the plasticity of ionocyte functions in the euryhaline teleost. Front Physiol 13:914277

Ishiguro H, Steward MC, Naruse S, Ko SB, Goto H, Case RM, Kondo T, Yamamoto A (2009) CFTR functions as a bicarbonate channel in pancreatic duct cells. J Gen Physiol 133:315–326

Johannsson OE, Bergman HL, Wood CM, Laurent P, Kavembe DG, Bianchini A, Maina JN, Chevalier C, Bianchini LF, Papah MB, Ojoo RO (2014) Air breathing in the Lake Magadi tilapia *Alcolapia grahami*, under normoxic and hyperoxic conditions, and the association with sunlight and ROS. J Fish Biol 84:844–863

Johansen K, Maloiy GMO, Lykkeboe G (1975) A fish in extreme alkalinity. Respir Physiol 24:156–162

Kavembe GD, Franchini P, Irisarri I, Machado-Schiaffino G, Meyer A (2015) Genomics of adaptation to multiple concurrent stresses: insights from comparative transcriptomics of a Cichlid fish from one of earth's most extreme environments, the hypersaline soda Lake Magadi in Kenya, East Africa. J Mol Evol 81:90–109

Kurita Y, Nakada T, Kato A, Doi H, Mistry AC, Chang MH, Romero MF, Hirose S (2008) Identification of intestinal bicarbonate transporters involved in formation of carbonate precipitates to stimulate water absorption in marine teleost fish. Am J Physiol 294(4):R1402–R1412

Laurent P, Maina JN, Bergman HL, Narahara N, Walsh PJ, Wood CM (1995) Gill structure of a fish from an alkaline lake: effect of short-term exposure to neutral conditions. Can. J. Zool 73:1170–1181

Laurent P, Wood CM, Wang Y, Perry SF, Gilmour KM, Pärt P, Walsh PJ (2000) A new type of intracellular vesicular trafficking in the gill of urea-excreting fish (*Opsanus* sp.) in the family Batrachoididae. Cell Tissue Res 303(2):197–210

LeMoine CM, Walsh PJ (2015) Evolution of urea transporters in vertebrates: adaptation to urea's multiple roles and metabolic sources. J. Exp. Biol. 218(12):1936–1945

Lindley TE, Scheiderer CL, Walsh PJ, Wood CM, Bergman HG, Bergman AN, Laurent P, Wilson P, Anderson PM (1999) Muscle as a primary site of urea cycle enzyme activity in an alkaline lake-adapted tilapia, *Oreochromis alcalicus grahami*. J Biol Chem 274:29858–29861

Linsdell P, Tabcharani JA, Rommens JM, Hou YX, Chang XB, Tsui LC, Riordan JR, Hanrahan JW (1997) Permeability of wild-type and mutant cystic fibrosis transmembrane conductance regulator chloride channels to polyatomic anions. J. Gen. Physiol. 110(4):355–364

Lytle C, Xu JC, Biemesderfer D, Forbush B III (1995) Distribution and diversity of Na–K–Cl cotransporter proteins: a study with monoclonal antibodies. Am J Physiol 269:C1496–C1505

Maina JN (1990) A study of the morphology of the gills of an extreme alkalinity and hyperosmotic adapted teleost *Oreochromis alcalicus grahami* (Boulenger) with particular emphasis on the ultrastructure of the chloride cells and their modifications with water dilution. A SEM and TEM study. Anat Embryol 181:83–98

Maina JN (1991) A morphometric analysis of chloride cells in the gills of the teleosts *Oreochromis alcalicus* and *Oreochromis niloticus* and a description of presumptive urea-excreting cells in *O. alcalicus*. J Anat 175:131–145

Maloiy GMO, Lykkeboe G, Johansen K, Bamford OS (1978) Osmoregulation in Tilapia grahami: a fish in extreme alkalinity. In: Schmidt-Nielsen K, Bolis L, Maddrell SHP (eds) Comparative Physiology: Water, Ions and Fluid Mechanics. Cambridge University Press, Cambridge, U.K., pp 229–238

Marshall WS, Lynch EM, Cozzi RRF (2002) Redistribution of immunofluorescence of CFTR anion channel and NKCC cotransporter in chloride cells during adaptation of the killifish Fundulus heteroclitus to sea water. J Exp Biol 205:1265–1273

Marshall WS, Singer TD (2002) Cystic fibrosis transmembrane conductance regulator in teleost fish. Biochimica Et Biophysica Acta (BBA) 1566(1–2):16–27

McCormick SD, Hasegawa S, Hirano T (1992) Calcium uptake in the skin of a freshwater teleost. Proc Natl Acad Sci U S A 89(8):3635–3638

Mistry AC, Honda S, Hirata T, Kato A, Hirose S (2001) Eel urea transporter is localized to chloride cells and is salinity dependent. Am J Physiol 281(5):R1594–R1604

Narahara A, Bergman HL, Laurent P, Maina JN, Walsh PJ, Wood CM (1996) Respiratory physiology of the Lake Magadi tilapia (Oreochromis alcalicus grahami), a fish adapted to a hot, alkaline, and frequently hypoxic environment. Physiol Zool 69:1114–1136

Potts WTW (1984) Transepithelial potentials in fish gills. In: Hoar WS, Randall DJ (eds) Fish Physiology, vol Vol 10B. Academic Press, Orlando, pp 105–128

Potts WTW, Hedges AJ (1991) Gill potentials in marine teleosts. J Comp Physiol B 161:401–405

Poulsen JH, Fischer H, Illek B, Machen TE (1994) Bicarbonate conductance and pH regulatory capability of Cystic fibrosis transmembrane conductance regulator. Proc Natl Acad Sci U S A 91(12):5340–5344

Randall DJ, Wood CM, Perry SF, Bergman HL, Maloiy GMO, Mommsen TP, Wright PA (1989) Urea excretion as a strategy for survival in a fish living in a very alkaline environment. Nature 337:165–166

Silva P, Soloman R, Spokes K, Epstein FH (1977) Ouabain inhibition of gill Na-K-ATPase: relationship to active chloride transport. J Exp Zool 199:419–426

Singer TD, Tucker SJ, Marshall WS, Higgins CF (1998) A divergent CFTR homologue: highly regulated salt transport in the euryhaline teleost *Fundulus heteroclitus*. Am J Physiol 274(3):C715–C723

Takeyasu K, Tamkun MM, Renaud KJ, Fambrough DM (1988) Ouabain-sensitive (Na++ K+)-ATPase activity expressed in mouse L cells by transfection with DNA encoding the alpha-subunit of an avian sodium pump. J Biol Chem 263:4347–4354

Takvam M, Wood CM, Kryvi H, Nilsen TO (2021) Ion transporters and osmoregulation in the kidney of teleost fishes as a function of salinity. Front Physiol 12:664588

Tang L, Fatehi M, Linsdell P (2009) Mechanism of direct bicarbonate transport by the CFTR anion channel. J Cyst Fibros 8:115–121

Ura K, Soyano K, Omoto N, Adachi S, Yamauchi K (1996) Localization of Na, K-ATPase in Tissues of Rabbit and Teleosts Using an Antiserum Directed Against a Partial Sequence of the α-Subunit. Zool Sci 13:219–227

Walsh PJ, Heitz M, Campbell CE, Cooper GJ, Medina M, Wang YS, Goss GG, Vincek V, Wood CM, Smith CP (2000) Molecular identification of a urea transporter in gill of the ureotelic gulf toadfish (*Opsanus beta*). J Exp Biol 203:2357–2364

Walsh PJ, Grosell M, Goss GG, Bergman HL, Bergman AN, Wilson P, Laurent P, Alper SL, Smith CP, Kamunde C, Wood CM (2001) Physiological and molecular characterization of urea transport by the gills of the Lake Magadi tilapia (*Alcolapia grahami*). J Exp Biol 204(3):509–520

Watanabe S, Niida M, Maruyama T, Kaneko T (2008) Na^+/H^+ exchanger isoform 3 expressed in apical membrane of gill mitochondrion-rich cells in Mozambique tilapia *Oreochromis mossambicus*. Fish Sci 74:813–821

Wilson JM (2007) The use of immunochemistry in the study of branchial ion transport mechanisms. In: Baldisserotto B, Mancera JM, Kapoor BG (eds) Fish osmoregulation. Science Publishers Inc., Enfield, pp 359–394

Wilson JM, Leitão A, Gonçalves AF, Ferreira C, Reis-Santos P, Fonseca AV, da Silva JM, Antunes JC, Pereira-Wilson C, Coimbra J (2007) Modulation of branchial ion transport protein expression by salinity in glass eels (*Anguilla anguilla* L.). Mar Biol 151:1633–1645

Wilson PJ, Wood CM, Walsh PJ, Bergman AL, Bergman HL, Laurent P, White BN (2004) Discordance between genetic structure and morphological, ecological, and physiological adaptation in Lake Magadi tilapia. Physiol Biochem Zool 77:537–555

Wood CM, Perry SF, Wright PA, Bergman HL, Randall DJ (1989) Ammonia and urea dynamics in the Lake Magadi tilapia, a ureotelic teleost fish adapted to an extremely alkaline environment. Respir Physiol Neurobiol 77:1–20

Wood CM, Bergman HL, Laurent P, Maina JN, Narahara A, Walsh P (1994) Urea production, acid-base regulation and their interactions in the Lake Magadi tilapia, a unique teleost adapted to a highly alkaline environment. J Exp Biol 189:13–36

Wood CM, Wilson PW, Bergman HL, Bergman AN, Laurent P, Otiang'a-Owiti G, Walsh PJ (2002a) Ionoregulatory strategies and the role of urea in the Magadi tilapia (*Alcolapia grahami*). Can J Zool 80:503–515

Wood CM, Wilson PW, Bergman HL, Bergman AN, Laurent P, Otiang'a-Owiti G, Walsh PJ (2002b) Obligatory urea production and the cost of living in the Magadi tilapia revealed by acclimation to reduced salinity and alkalinity. Physiol Biochem Zool 75:111–122

Wood CM, Bergman HL, Bianchini A, Laurent P, Maina J, Johannsson OE, Bianchini LF, Chevalier C, Kavembe GD, Papah MB, Ojoo RO (2012) Transepithelial potential in Magadi tilapia, a fish in extreme alkalinity. J Comp Physiol B 182:247–258

Wood CM, Nawata CM, Wilson JM, Laurent P, Chevalier C, Bergman HL, Bianchini A, Maina JN, Johannson OE, Bianchini LF, Kavembe GD, Papah MB, Ojoo RO (2013) Rh proteins and NH_4^+-activated Na^+ATPase in the Magadi tilapia (*Alcolapia grahami*), a 100% ureotelic teleost fish. J Exp Biol 216:2998–3007

Wood CM, Brix KV, De Boeck G, Bergman HL, Bianchini A, Bianchini LF, Maina JN, Johannsson OE, Kavembe GD, Papah MB, Letura KM, Ojoo RO (2016) Mammalian metabolic rates in the hottest fish on earth. Sci Rep 6:26990

Wright PA, Wood CM, Hiroi J, Wilson JM (2016) (Uncommon) mechanisms of branchial ammonia excretion in the common carp (Cyprinus carpio) in response to environmentally induced metabolic acidosis. Physiol Biochem Zool 89:26–40

Wright PA, Wood CM, Wilson JM (2014) Rh versus pH: the role of Rhesus glycoproteins in renal ammonia excretion during metabolic acidosis in a freshwater teleost fish. J Exp Biol 217:2855–2865

Zhang Y, Zhang C, Dong Y, Li P, Chen Z, Qi X, Wen H, Wang L, Li Y (2026) Integrated transcriptomic and physiological analyses uncover multi-organ strategies of spotted sea bass (*Lateolabrax maculatus*) for alkalinity adaptation. Aquaculture 618:743793

Zhao Y, Zhang C, Zhou H, Song L, Wang J, Zhao J (2020) Transcriptome changes for Nile tilapia (*Oreochromis niloticus*) in response to alkalinity stress. Comp Biochem Physiol D Genomics Proteomics 33:100651

Publisher's Note Springer Nature remains neutral with regard to jurisdictional claims in published maps and institutional affiliations.

Springer Nature or its licensor (e.g. a society or other partner) holds exclusive rights to this article under a publishing agreement with the author(s) or other rightsholder(s); author self-archiving of the accepted manuscript version of this article is solely governed by the terms of such publishing agreement and applicable law.